

Supplementary Information for:

## **Structure of a model TiO<sub>2</sub> photocatalytic interface**

H. Hussain<sup>1,2†</sup>, G. Tocci<sup>1</sup>, T. Woolcot<sup>1</sup>, X. Torrelles<sup>3</sup>, C. L. Pang<sup>1</sup>, D. S. Humphrey<sup>1</sup>,  
C. M. Yim<sup>1</sup>, D. C. Grinter<sup>1§</sup>, G. Cabailh<sup>4,5</sup>, O. Bikondoa<sup>6</sup>, R. Lindsay<sup>7</sup>, J.  
Zegenhagen<sup>2‡</sup>, A. Michaelides<sup>1</sup>, G. Thornton<sup>1\*</sup>

<sup>1</sup> London Centre for Nanotechnology and Department of Chemistry, University  
College London, 20 Gordon Street, London WC1H 0AJ, UK.

<sup>2</sup> ESRF, 6 rue Jules Horowitz, F-38000 Grenoble cedex, France.

<sup>3</sup> Institut de Ciència de Materials de Barcelona (CSIC), Campus UAB, 08193  
Bellaterra, Spain.

<sup>4</sup> Sorbonne Universités, UPMC Univ Paris 06, CNRS, 75005 Paris, France.

<sup>5</sup> CNRS, UMR 7588, Institut des NanoSciences de Paris, 75005 Paris, France.

<sup>6</sup> Department of Physics, University of Warwick, Gibbet Hill Road, Coventry C4  
7AL, UK.

<sup>7</sup> Corrosion and Protection Centre, School of Materials, The University of  
Manchester, Sackville Street, Manchester, M13 9PL, UK.

\* To whom correspondence should be addressed. Email: [g.thornton@ucl.ac.uk](mailto:g.thornton@ucl.ac.uk)

Current Addresses:

† Corrosion and Protection Centre, School of Materials, The University of  
Manchester, Sackville Street, Manchester, M13 9PL, UK.

§ Chemistry Department, Building 555, Brookhaven National Laboratory, Upton, NY  
11973, USA.

‡ Diamond Light Source Ltd., Diamond House, Harwell Science and Innovation  
Campus, Didcot, Oxfordshire, OX11 0DE, UK.

\*To whom correspondence should be addressed. Email [g.thornton@ucl.ac.uk](mailto:g.thornton@ucl.ac.uk)

This pdf file contains:

Figures S1-S11

Tables S1, S2

Movie S1

References

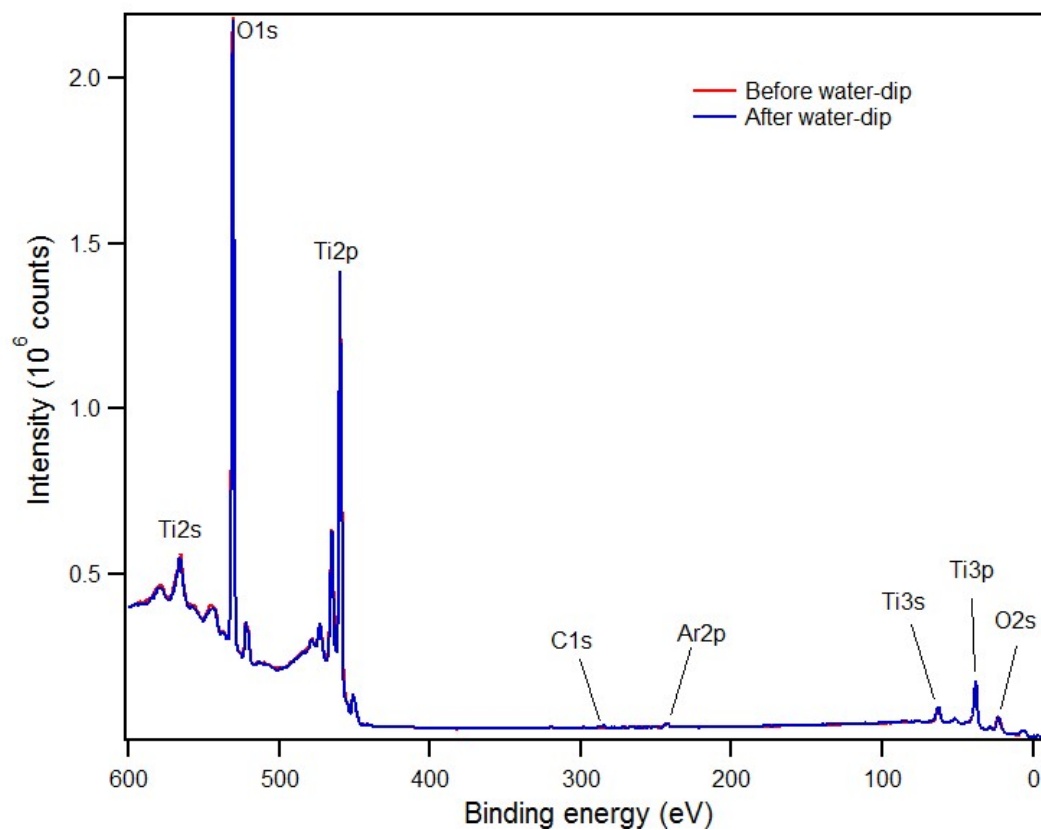


**Fig. S1 | XPS spectra from  $\text{TiO}_2(110)/\text{H}_2\text{O}_{\text{dip}}$ . Al  $\text{K}\alpha$  ( $h\nu = 1486.6$  eV)**

photoelectron spectra recorded at normal emission from as-prepared  $\text{TiO}_2(110)$  and from the sample following immersion in liquid water. Analysis of the  $\text{H}_2\text{O}_{\text{dip}}$  spectrum using the methodology in Ref. 1 indicates a C coverage of 0.1 ML.

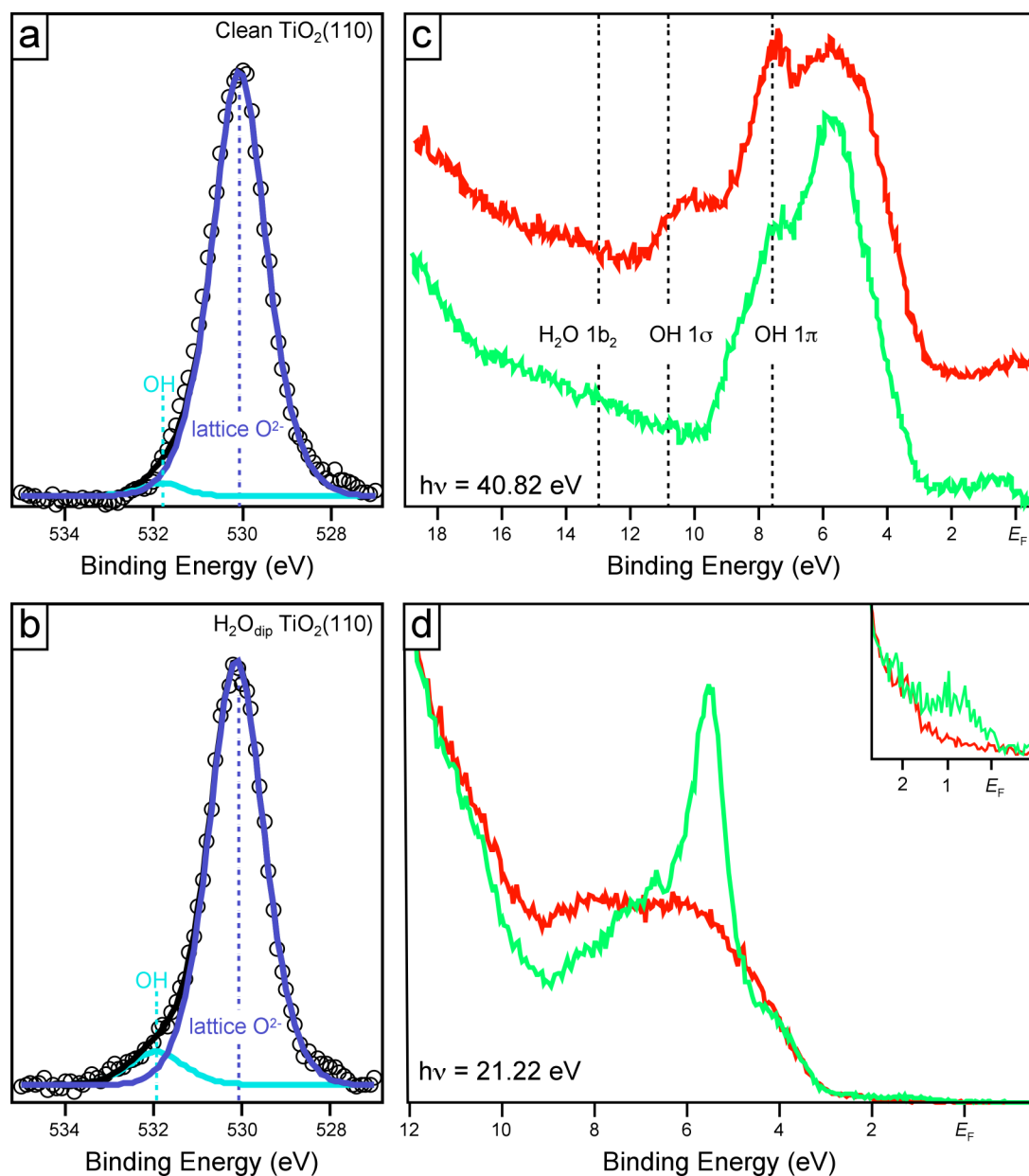


**Fig. S2 | Photoemission spectra associated with the  $\text{H}_2\text{O}_{\text{dip}}$  sample.** **a**, Al  $\text{K}\alpha$  ( $h\nu = 1486.6$  eV) photoelectron spectra taken at normal emission from the as-prepared  $\text{TiO}_2(110)$  and **b**, the  $\text{H}_2\text{O}_{\text{dip}}$  sample after immersion in liquid water. The peaks were fitted using Gaussian-Lorentzian line shapes after removal of a Shirley background. Peaks are present at  $\sim 530$  eV and 532 eV which arise from lattice oxygen and OH, respectively<sup>2</sup>. Molecular water, if it were present would appear at  $\sim 534$  eV (Ref. 2). We note that X-ray induced beam damage is not expected on the basis of earlier work



which reported a photoemission study of  $\text{TiO}_2(110)\text{-H}_2\text{O}$  (Ref. 3). **c**, He II ( $h\nu = 40.82$  eV) photoemission spectra taken from the as-prepared surface before (green) and after (red) immersion in liquid water to form the  $\text{H}_2\text{O}_{\text{dip}}$  surface. The spectra are offset for clarity and the spectrum from the  $\text{H}_2\text{O}_{\text{dip}}$  sample is corrected for band bending. The positions of the OH  $3\sigma$  and  $1\pi$  peaks, as well as the absent  $\text{H}_2\text{O } 1b_2$  peak position, are marked with dashed lines<sup>4</sup>. **d**, He I ( $h\nu = 21.22$  eV) photoemission spectra taken from the as-prepared surface before (green) and after (red) immersion in liquid water to form the  $\text{H}_2\text{O}_{\text{dip}}$  surface. The  $\text{H}_2\text{O}_{\text{dip}}$  spectrum is corrected for band bending. The inset shows an expanded view of the band gap region and indicates that after immersion in water, the BGS is quenched.

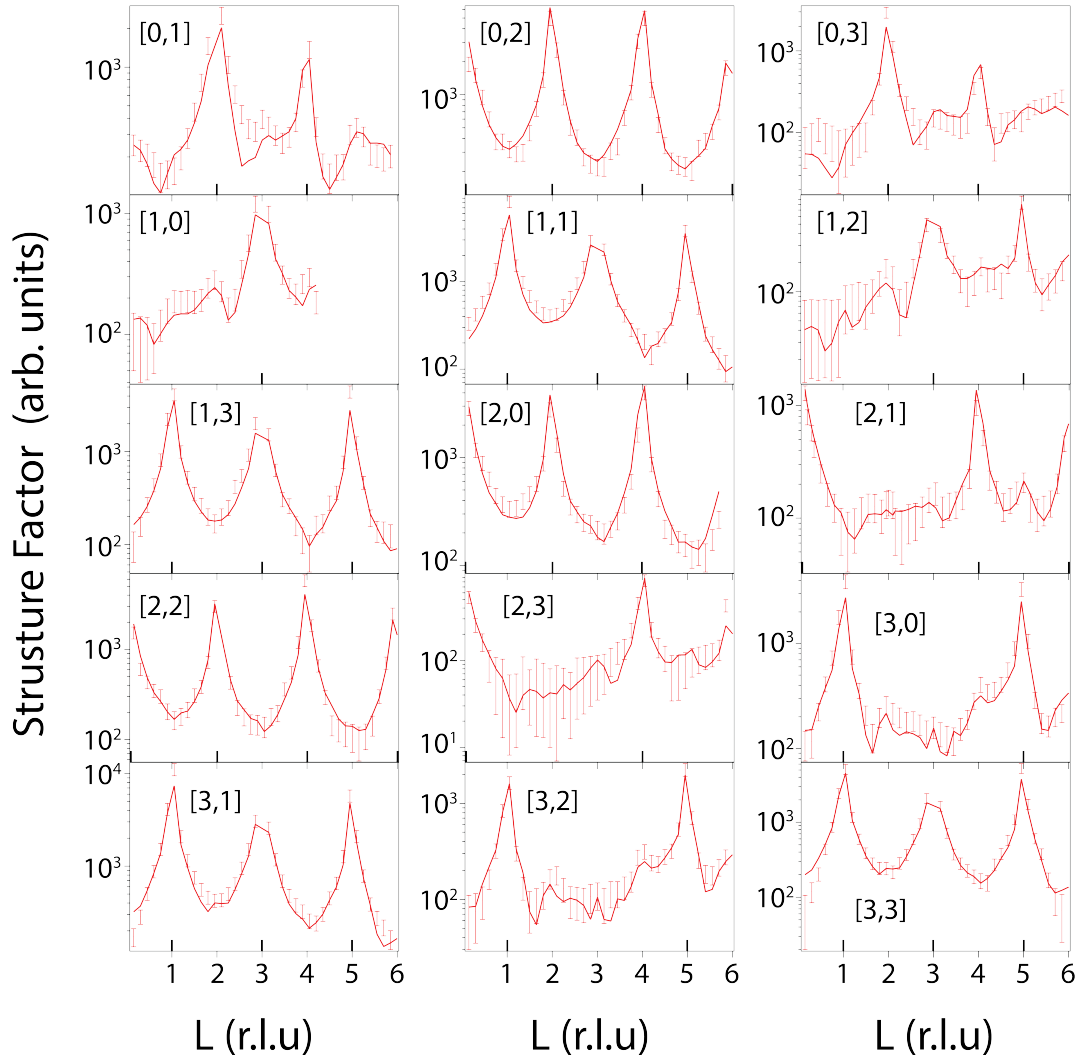
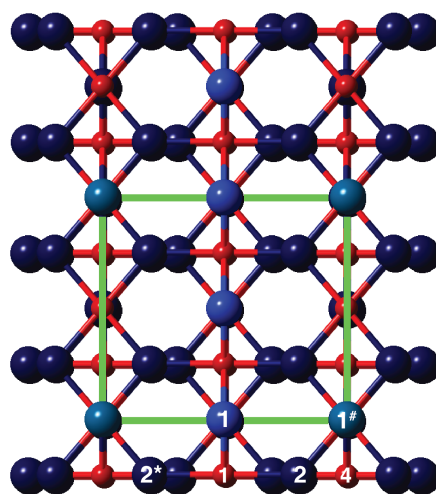
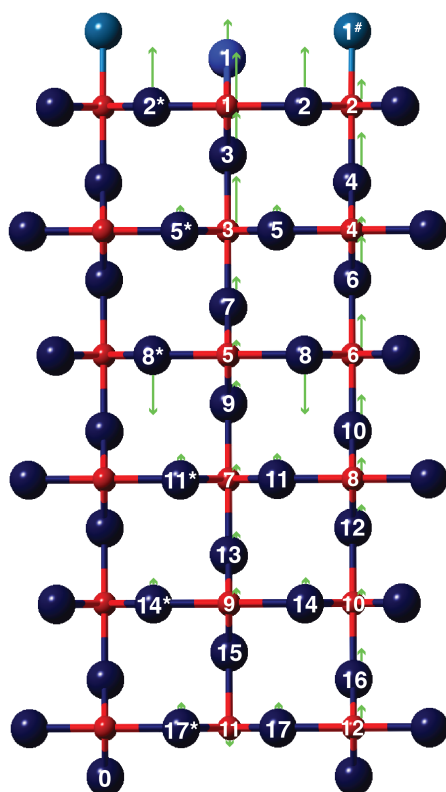


**Fig. S3 | Representative CTRs measured for the  $\text{H}_2\text{O}_{\text{dip}}$  experiment.** Error bars are the experimental data and the solid lines are the corresponding best fits to the data. Notches on the  $x$  axes correspond to Bragg peaks.

a



b

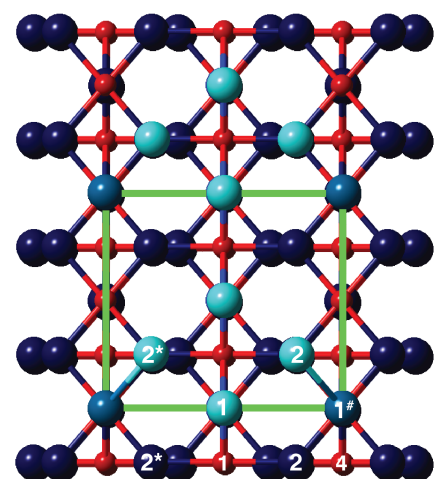
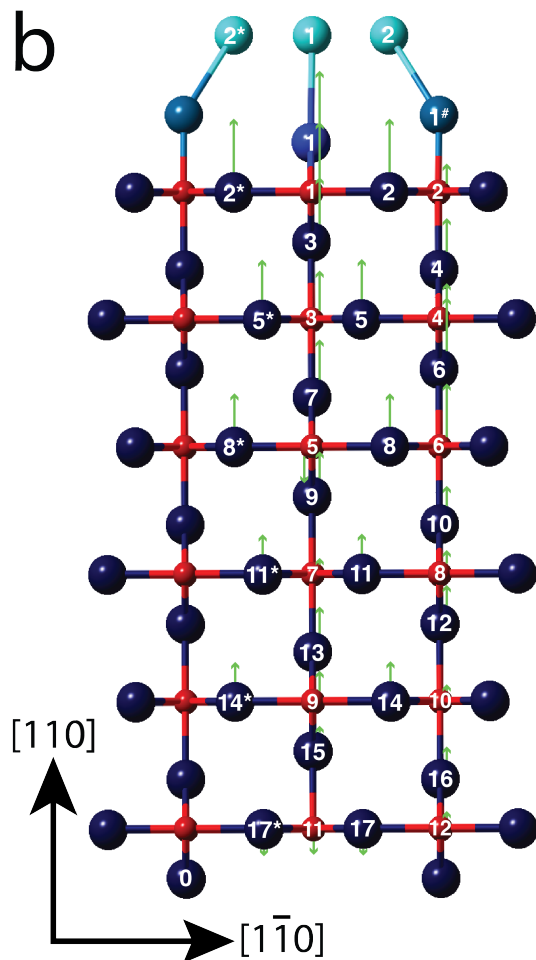


**Fig. S4 | Best-fit ball and stick models determined from the SXRD data viewed along [001] and [110].** Large blue spheres are oxygen atoms, small red spheres are titanium atoms. O nearer the surface are shaded lighter, H<sub>2</sub>O atoms the lightest. Green arrows represent the direction and magnitude of atomic displacements away from the bulk structure. Hydrogen atoms are purposely left out due to their low X-ray scattering factor. The numerical labeling of atoms is employed in Supplementary Table S1 and S2 for identification purposes. Symmetry-paired atoms are denoted as 2\*, 5\*, 8\*, 11\*, 14\* and 17\*. **a**, The OH<sub>t</sub> model for the H<sub>2</sub>O<sub>dip</sub> sample and **b**, the hydrated model for the H<sub>2</sub>O<sub>drop</sub> sample. Green line indicates the (2x1) unit cell. Atom O1<sup>#</sup> represents the OH<sub>t</sub> molecule.

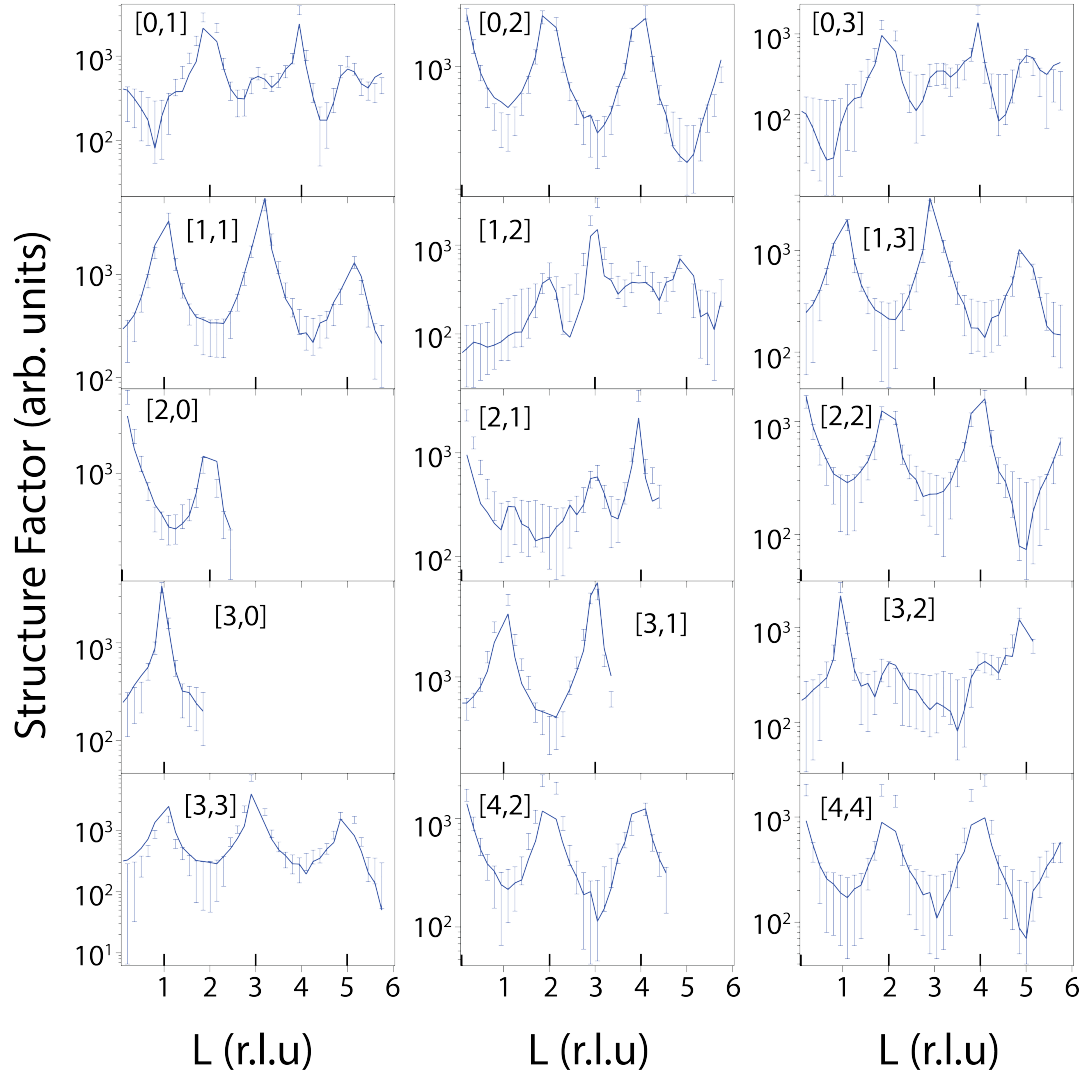


**Fig. S5 | Representative CTRs measured for the  $\text{H}_2\text{O}_{\text{drop}}$  experiment.** Blue error bars are the experimental data and solid blue lines are the corresponding best fits to the data. Notches on the  $x$  axes correspond to Bragg peaks.

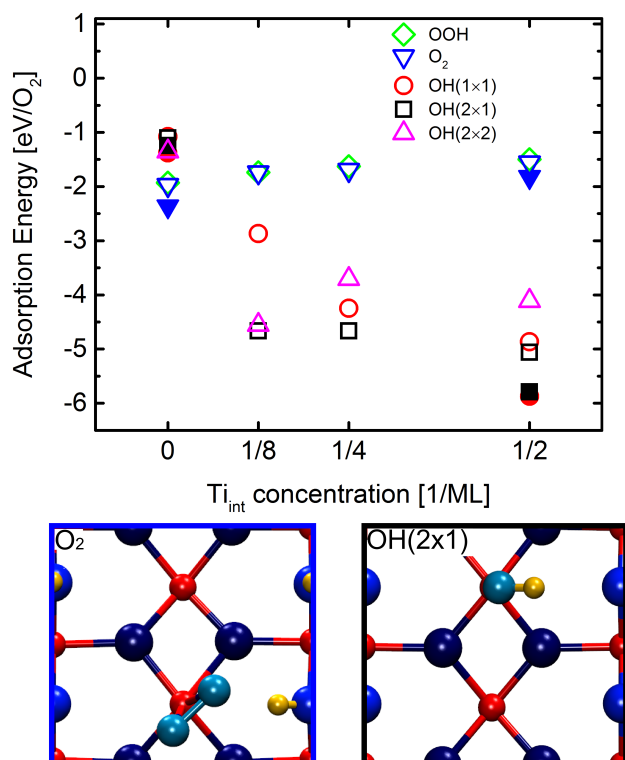


**Fig. S6 Stability of overlayer as a function of  $Ti_{int}$  concentration.** Adsorption energy of  $O_2$  on a hydroxylated  $TiO_2(110)$  surface at different  $Ti_{int}$  concentrations. Without interstitials the adsorption of  $O_2$  or of a peroxy group (OOH) is more favorable than the dissociation to  $OH_t$ . At  $Ti_{int}$  concentrations of 1/8 ML or larger the  $OH_t$  overlayer is more stable. Specifically, between 1/8 and 1/4 ML of  $Ti_{int}$  the  $OH_t(2 \times 1)$  overlayer is the most stable structure. At a concentration of 1/2 ML the  $OH_t(1 \times 1)$  overlayer is the most stable structure. At a concentration of 1/2 ML the  $OH_t(1 \times 1)$  becomes instead the most stable structure. This concentration, however, is likely too large to be observed experimentally. The data at 1/2 ML is shown to compare to HSE<sup>5</sup> results (filled symbols). Empty symbols are results obtained using PBE+U<sup>6,7</sup>, with a value of  $U_{s3} = 4.2$  eV. Snapshots at the bottom indicate the two adsorption structures for the  $OH_t(2 \times 1)$  overlayer and the  $O_2$  overlayer with the frames in the same colours used for the symbols in the graph.

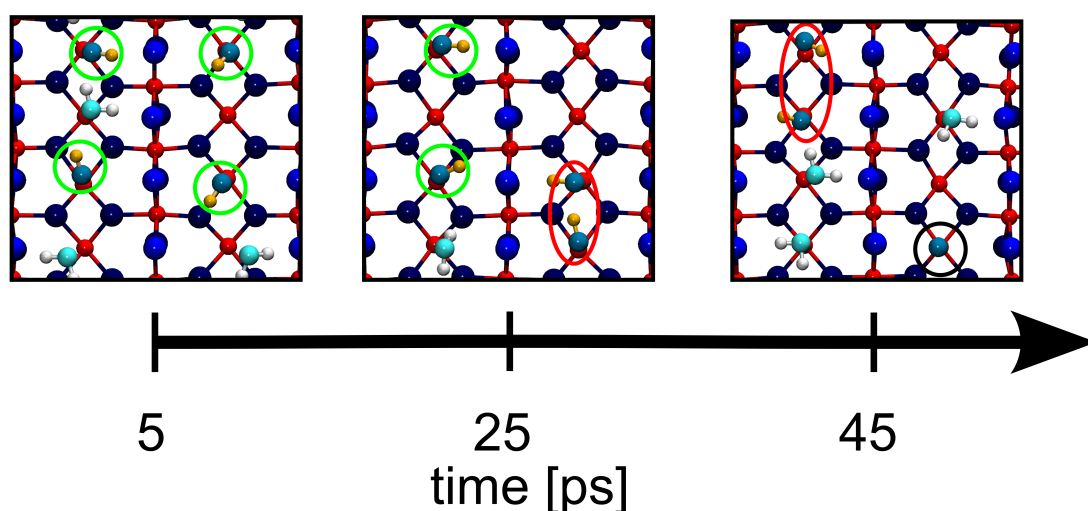


**Fig. S7 | Instability of  $\text{OH}_t(2 \times 1)$  overlayer without interstitials.** Time evolution of a contact layer of hydroxide  $\text{OH}^-$  on defect-free  $\text{TiO}_2(110)$  under aqueous conditions obtained from AIMD. The snapshots show that the  $(2 \times 1)$  symmetry of the  $\text{OH}_t$  overlayer is disrupted over the time of the simulation due to a sequence of proton transfer reactions involving the  $\text{OH}$  species and water. The  $(2 \times 1)$  symmetry, apparent at the beginning of the AIMD trajectory (5 ps), is already broken after 25 ps, as an  $\text{OH}$  dimer is formed. Before 45 ps a proton hops from one of the two  $\text{OH}_t$  on to the other to form water, leaving an O-atom adsorbed on a  $\text{Ti}_{5c}$ . Another  $\text{OH}_t$  dimer structure also forms, disrupting completely the initial symmetry. The green circles indicate single  $\text{OH}_t$  species, while red circles are drawn around adjacent  $\text{OH}_t$  species and black ones around the O-atom. Water molecules above the contact layer are not shown.

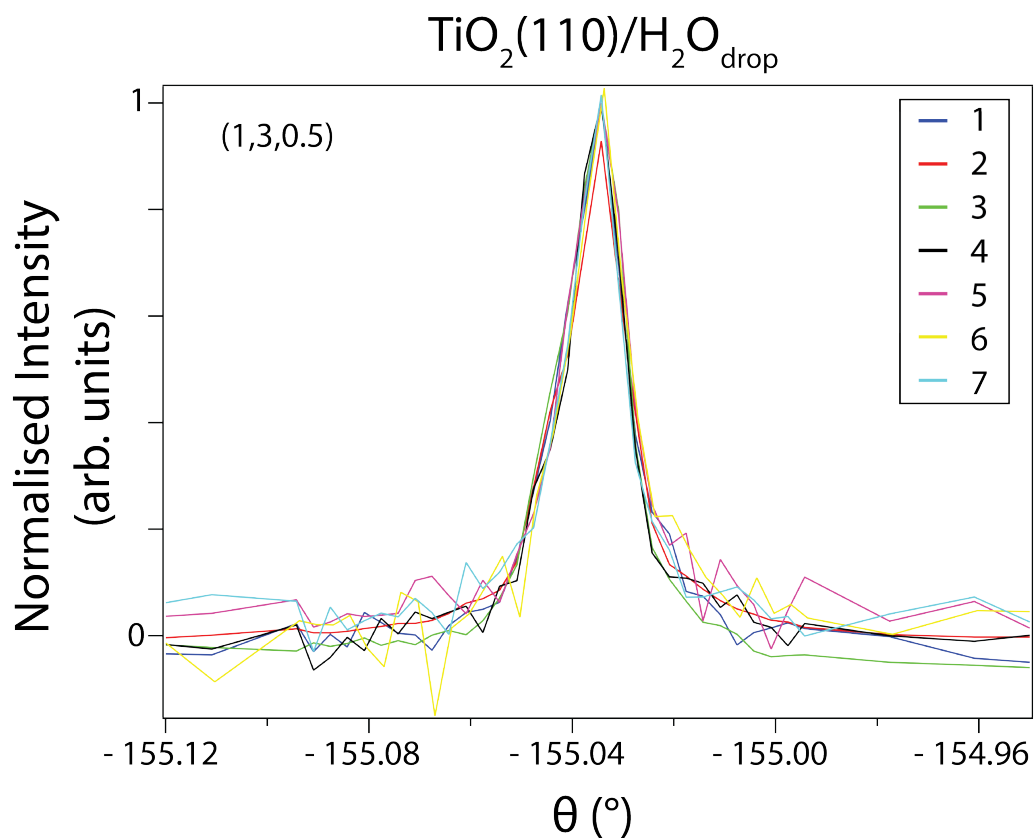


**Fig. S8 | Monitoring the stability of the  $\text{TiO}_2(110)\text{-H}_2\text{O}_{\text{drop}}$  surface structure.**

Reference  $(1,3,0.5)$  reflections from  $\text{TiO}_2(110)\text{-H}_2\text{O}_{\text{drop}}$  recorded as  $\theta$  scans at an average 5 hour intervals in the sequence 1-7, starting from time zero. The complete CTR dataset for this surface was recorded in 25 hours.



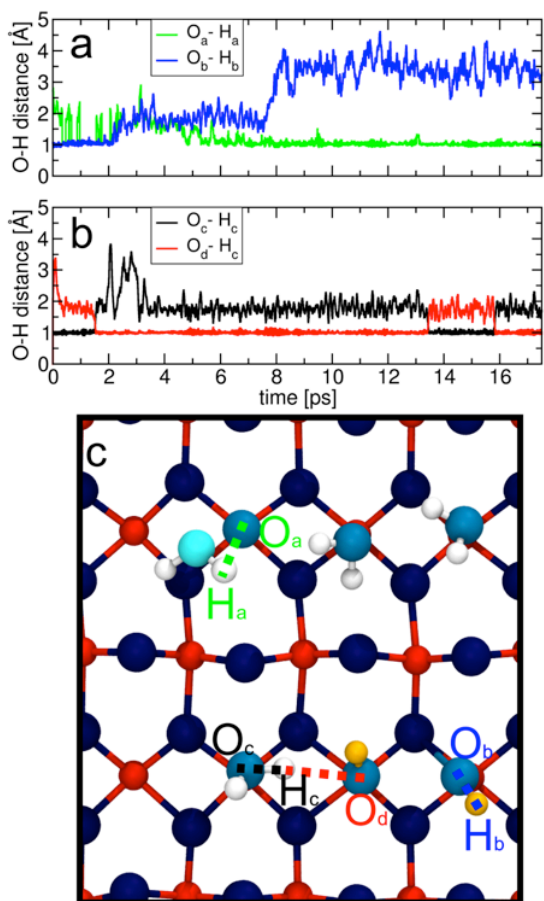


**Fig. S9 | Facile proton transfer reactions in the  $2OH_t+O_{ad}$  overlayer.** Time evolution of the distances between several O atoms and H atoms that are involved in different proton transfer reactions, as obtained from a 17.5 ps-long AIMD simulation of a  $TiO_2(110)$  surface under aqueous conditions and with  $1/4$  ML  $Ti_{int}$ . Time evolution of the distances between O atoms and H atoms, in which the protons diffuse to/from the liquid (a), or hop between two neighbouring O atoms (b). The starting configuration of the contact layer consists of  $1/8$  ML  $O_{ad}$  and two adjacent  $OH_t$  at a coverage of  $1/4$ ML shown in top view (c). In the figures (a) and (b), the protons are bonded to the corresponding O atom when the O-H distances are around  $1.0 \text{ \AA}$ . The dotted lines and the atom labels in c are colour-coded according to the graphs of figures (a) and (b).

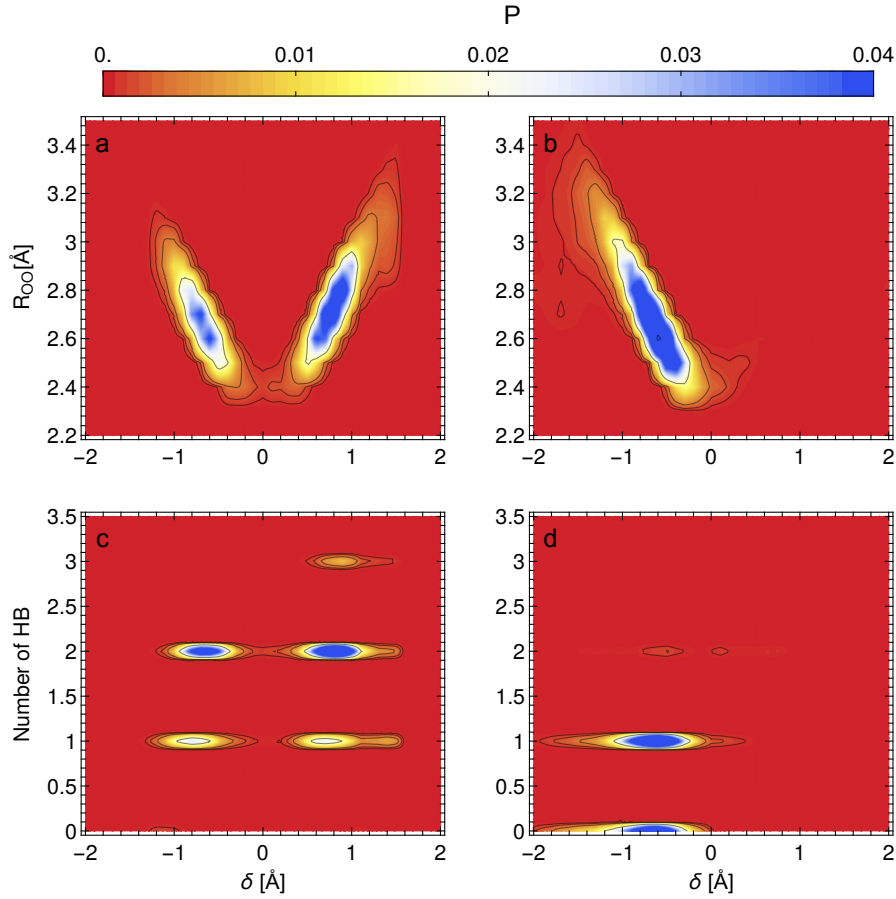


**Fig. S10 | Facile proton transfer dynamics in the  $2\text{OH}_t + \text{O}_{\text{ad}}$  overlayer compared to the  $\text{OH}_t(2 \times 1)$  overlayer.** Contour plots of the probability distribution for protons hopping between two oxygen atoms, as a function of the O-O distance  $R_{OO}$  and of the proton displacement  $\delta$  with respect to the two neighbouring oxygen atoms for (a) the  $2\text{OH}_t + \text{O}_{\text{ad}}$  overlayer and (b) the  $\text{OH}_t(2 \times 1)$  overlayer.  $\delta$  is defined here as  $R_{O_a H} - R_{O_b H}$ , where  $O_a$  is the oxygen atom that in the initial configuration of the AIMD simulation belongs to an  $\text{OH}_t$  or an  $\text{O}_{\text{ad}}$  species and  $O_b$  is the oxygen of a specie that is nearest to  $O_a$ . (c) and (d): Probability distribution as a function of  $\delta$  and of the number of hydrogen bonds associated with the oxygen  $O_a$  and computed according to the geometric criterion of Ref. 8 for the  $2\text{OH}_t + \text{O}_{\text{ad}}$  and the  $\text{OH}_t(2 \times 1)$  overlayer, respectively. It can be seen that proton transfer is more facile at the  $2\text{OH}_t + \text{O}_{\text{ad}}$  overlayer (see Fig. S9(b)) compared to the  $\text{OH}_t(2 \times 1)$  overlayer. The hopping (or

not) of the protons in the two configurations is correlated to the distribution of H-bonds that the  $\text{OH}_t$  and the  $\text{O}_{ad}$  species engage in with the surrounding molecules. The analysis has been carried out on a total of 4 AIMD trajectories that have been started from different initial conditions. The two trajectories for the  $2\text{OH}_t + \text{O}_{ad}$  overlayer, each of which is about 20 ps-long, while the ones for the  $\text{OH}_t(2 \times 1)$  overlayer are 50 ps-long and 20 ps-long.

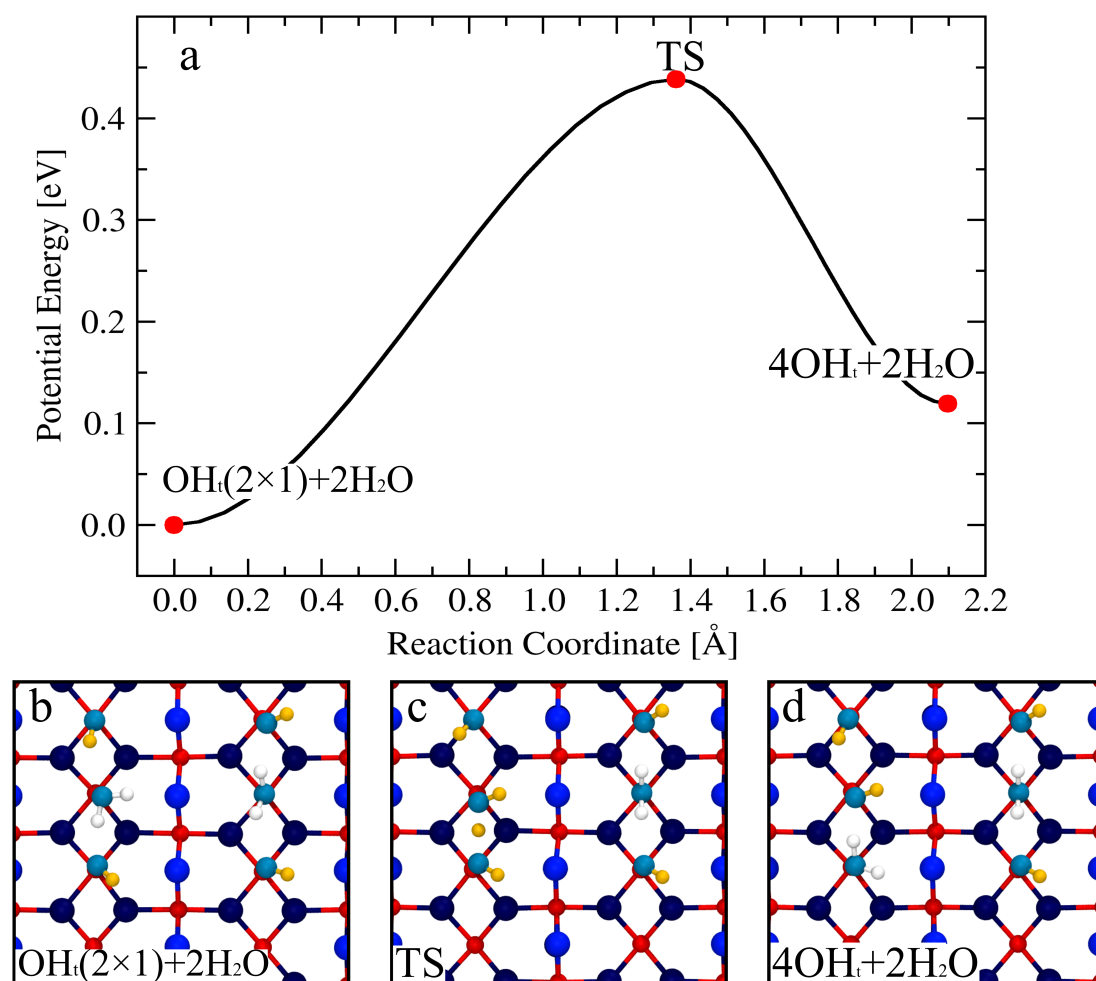


**Fig. S11 | Energy path for the hopping of a proton from an  $\text{H}_2\text{O}$  to an  $\text{OH}_t$  at the  $\text{OH}_t(2 \times 1) + 2\text{H}_2\text{O}$  overlayer.** (a) Potential energy diagram computed with CP2K with the PBE0-TC-LR functional<sup>9,10,11</sup>. The transition state has been computed using the climbing image nudged elastic band method.<sup>12</sup> (b)-(d): Snapshots of the  $\text{OH}_t(2 \times 1)$

1)+2H<sub>2</sub>O overlayer (i.e. energy zero reference state), of the TS, and of the disordered 4OH<sub>t</sub>+2H<sub>2</sub>O overlayer (i.e the final state), respectively. It can be seen that the OH<sub>t</sub>(2 x 1) + 2H<sub>2</sub>O overlayer is about 0.10 eV more stable than the 4OH<sub>t</sub> + 2H<sub>2</sub>O overlayer and that there is a barrier of about 0.43 eV for this transition.

**Supplementary Table S1** SXRD-derived substrate atomic displacements (Å) away from the bulk-terminated structure for the H<sub>2</sub>O<sub>dip</sub> and H<sub>2</sub>O<sub>drop</sub> samples. Also listed are the displacements for the as-prepared UHV TiO<sub>2</sub>(110) surface prior to the H<sub>2</sub>O<sub>drop</sub> experiment (UHV<sub>as-prepared</sub>), values for previous SXRD measurements of TiO<sub>2</sub>(110) in UHV<sup>13</sup>, as well as the bulk truncated coordinates for TiO<sub>2</sub>(110)(1×1). It should be noted that the displacements given for the H<sub>2</sub>O<sub>dip</sub> and H<sub>2</sub>O<sub>drop</sub> samples are for the case where OH is adsorbed to surface Ti atoms. Unoccupied surface Ti atoms displace in quantitative agreement with the UHV<sub>as-prepared</sub> sample (see Methods). Supplementary Fig. S4 provides a key to the identity of the atoms. A negative value indicates that the atom moves towards the bulk for a displacement perpendicular to the surface plane, that is in the [110] direction, and in the [1 $\bar{1}$ 0] direction for a lateral displacement.

Atom	(1×1) Bulk Terminated Coordinates (Å)	Displacements (Å)			
		Ref. 13	UHV <sub>as-prepared</sub>	H <sub>2</sub> O <sub>(l)-dip</sub>	H <sub>2</sub> O <sub>(l)-drop</sub>
O(1)	18.77	0.10 ± 0.04	0.10 ± 0.04	0.03 ± 0.03	0.08 ± 0.04
O(2) [110]	17.50	0.17 ± 0.03	0.13 ± 0.03	0.06 ± 0.03	0.08 ± 0.03
O(2) [1 $\bar{1}$ 0]	5.23	0.01 ± 0.05	0.02 ± 0.04	0.01 ± 0.05	0.01 ± 0.05
Ti(1)	17.50	0.25 ± 0.01	0.17 ± 0.01	0.07 ± 0.01	0.09 ± 0.01
Ti(2)	17.50	-0.11 ± 0.01	-0.06 ± 0.01	0.03 ± 0.01	0.03 ± 0.01
O(3)	16.24	0.07 ± 0.04	0.07 ± 0.04	0.04 ± 0.04	0.07 ± 0.03
O(4)	15.52	0.00 ± 0.03	0.02 ± 0.03	0.05 ± 0.03	0.05 ± 0.05
O(5) [110]	14.25	0.04 ± 0.03	0.03 ± 0.03	0.01 ± 0.03	0.06 ± 0.03
O(5) [1 $\bar{1}$ 0]	4.37	0.05 ± 0.05	0.02 ± 0.03	0.03 ± 0.03	0.05 ± 0.05
Ti(3)	14.25	-0.08 ± 0.01	-0.02 ± 0.01	0.07 ± 0.01	0.06 ± 0.01
Ti(4)	14.25	0.19 ± 0.01	0.12 ± 0.01	0.01 ± 0.01	0.04 ± 0.01
O(6)	12.99	0.01 ± 0.04	0.04 ± 0.04	0.04 ± 0.03	0.08 ± 0.05

O(7)	12.27	$0.00 \pm 0.04$	$0.01 \pm 0.04$	$0.02 \pm 0.03$	$0.06 \pm 0.05$
O(8) [110]	11.01	$0.01 \pm 0.03$	$0.01 \pm 0.05$	$-0.06 \pm 0.03$	$0.05 \pm 0.03$
O(8) [ $1\bar{1}0$ ]	5.23	$-0.03 \pm 0.05$	$-0.02 \pm 0.05$	$-0.01 \pm 0.05$	$-0.03 \pm 0.02$
Ti(5)	11.01	$0.08 \pm 0.01$	$0.05 \pm 0.01$	$0.01 \pm 0.01$	$-0.04 \pm 0.01$
Ti(6)	11.01	$-0.04 \pm 0.01$	$-0.02 \pm 0.01$	$0.05 \pm 0.01$	$0.08 \pm 0.01$
O(9)	9.74	$0.02 \pm 0.04$	$0.03 \pm 0.03$	$0.01 \pm 0.03$	$0.04 \pm 0.04$
O(10)	9.02	$-0.02 \pm 0.04$	$-0.01 \pm 0.03$	$0.03 \pm 0.03$	$0.03 \pm 0.03$
O(11) [110]	7.76	$0.01 \pm 0.03$	$0.01 \pm 0.02$	$0.01 \pm 0.03$	$0.03 \pm 0.03$
O(11) [ $1\bar{1}0$ ]	4.37	$0.01 \pm 0.04$	$0.01 \pm 0.03$	$0.01 \pm 0.03$	$0.02 \pm 0.04$
Ti(7)	7.76	$-0.02 \pm 0.01$	$-0.01 \pm 0.01$	$0.01 \pm 0.01$	$0.01 \pm 0.01$
Ti(8)	7.76	$0.07 \pm 0.01$	$0.04 \pm 0.01$	$0.02 \pm 0.01$	$0.02 \pm 0.01$
O(12)	6.50	$0.02 \pm 0.02$	$0.02 \pm 0.03$	$0.01 \pm 0.02$	$0.03 \pm 0.04$
O(13)	5.78	$0.00 \pm 0.02$	$0.01 \pm 0.03$	$0.01 \pm 0.02$	$0.04 \pm 0.04$
O(14) [110]	4.51	$0.03 \pm 0.03$	$0.03 \pm 0.03$	$0.01 \pm 0.04$	$0.03 \pm 0.03$
O(14) [ $1\bar{1}0$ ]	5.23	$-0.02 \pm 0.03$	$-0.01 \pm 0.02$	$-0.01 \pm 0.03$	$-0.02 \pm 0.04$
Ti(9)	4.51	$0.02 \pm 0.01$	$0.01 \pm 0.01$	$0.01 \pm 0.01$	$0.03 \pm 0.01$
Ti(10)	4.51	$-0.01 \pm 0.01$	$-0.01 \pm 0.01$	$0.01 \pm 0.01$	$0.01 \pm 0.01$
O(15)	3.25	$0.00 \pm 0.02$	$0.01 \pm 0.03$	$0.00 \pm 0.02$	$0.01 \pm 0.02$
O(16)	2.53	$-0.02 \pm 0.02$	$-0.02 \pm 0.03$	$0.02 \pm 0.03$	$0.02 \pm 0.02$
O(17) [110]	1.26	$0.01 \pm 0.02$	$0.02 \pm 0.02$	$0.01 \pm 0.03$	$-0.01 \pm 0.03$
O(17) [ $1\bar{1}0$ ]	4.37	$0.02 \pm 0.02$	$0.01 \pm 0.02$	$0.01 \pm 0.02$	$0.02 \pm 0.02$
Ti(11)	1.26	$-0.01 \pm 0.01$	$-0.01 \pm 0.01$	$-0.01 \pm 0.01$	$-0.02 \pm 0.01$
Ti(12)	1.26	$0.03 \pm 0.01$	$0.01 \pm 0.01$	$0.00 \pm 0.01$	$0.01 \pm 0.01$

**Supplementary Table S2** SXRD-derived optimised locations of atoms (Å) relative to the position of O(0) at (0,0,0) for the H<sub>2</sub>O<sub>dip</sub> and H<sub>2</sub>O<sub>drop</sub> samples (see Supplementary Fig. S4 for a key to the identity of the atoms). Also listed are the atomic positions for the as-prepared UHV TiO<sub>2</sub>(110) surface prior to the H<sub>2</sub>O<sub>drop</sub> experiment (UHV<sub>as-prepared</sub>), values for previous SXRD measurements of TiO<sub>2</sub>(110) in UHV<sup>13</sup>, as well as the bulk truncated coordinates for TiO<sub>2</sub>(110)(1×1). The O atoms in OH and H<sub>2</sub>O are underlined in the table to highlight the fact that the positional parameters given are only for these atoms in the molecules.

Atom	(1×1) Bulk Terminated Coordinates (Å)	Optimised Positions (Å)			
		Ref. 13	UHV <sub>as-prepared</sub>	H <sub>2</sub> O <sub>(l)-dip</sub>	H <sub>2</sub> O <sub>(l)-drop</sub>
H <sub>2</sub> <u>O</u> (2) [110]	-	-	-	-	21.35
H <sub>2</sub> <u>O</u> (2) [ $\bar{1}\bar{1}0$ ]	-	-	-	-	5.32
H <sub>2</sub> <u>O</u> (1)	-	-	-	-	21.34
<u>OH</u> (1 <sup>#</sup> )	-	-	-	19.52	19.54
O(1)	18.77	18.87	18.87	18.80	18.85
O(2) [110]	17.50	17.67	17.63	17.56	17.58
O(2) [ $\bar{1}\bar{1}0$ ]	5.23	5.24	5.25	5.24	5.24
Ti(1)	17.50	17.75	17.67	17.57	17.59
Ti(2)	17.50	17.39	17.44	17.53	17.53
O(3)	16.24	16.31	16.31	16.28	16.31
O(4)	15.52	15.52	15.54	15.57	15.57
O(5) [110]	14.25	14.29	14.28	14.26	14.31
O(5) [ $\bar{1}\bar{1}0$ ]	4.37	4.42	4.39	4.40	4.42
Ti(3)	14.25	14.17	14.23	14.32	14.31
Ti(4)	14.25	14.44	14.37	14.26	14.29
O(6)	12.99	13.00	13.03	13.03	13.07
O(7)	12.27	12.27	12.28	12.29	12.33

O(8) [110]	11.01	11.02	11.02	10.95	11.06
O(8) [ $1\bar{1}0$ ]	5.23	5.20	5.21	5.22	5.20
Ti(5)	11.01	11.09	11.06	11.02	10.97
Ti(6)	11.01	10.97	10.99	11.06	11.09
O(9)	9.74	9.76	9.77	9.75	9.78
O(10)	9.02	9.00	9.01	9.05	9.05
O(11) [110]	7.76	7.77	7.77	7.77	7.79
O(11) [ $1\bar{1}0$ ]	4.37	4.38	4.38	4.38	4.39
Ti(7)	7.76	7.74	7.75	7.77	7.77
Ti(8)	7.76	7.83	7.80	7.78	7.78
O(12)	6.50	6.52	6.52	6.51	6.53
O(13)	5.78	5.78	5.79	5.79	5.82
O(14) [110]	4.51	4.54	4.54	4.52	4.54
O(14) [ $1\bar{1}0$ ]	5.23	5.21	5.22	5.22	5.21
Ti(9)	4.51	4.53	4.52	4.52	4.54
Ti(10)	4.51	4.50	4.50	4.52	4.52
O(15)	3.25	3.25	3.26	3.25	3.26
O(16)	2.53	2.51	2.51	2.55	2.55
O(17) [110]	1.26	1.27	1.28	1.27	1.25
O(17) [ $1\bar{1}0$ ]	4.37	4.39	4.38	4.38	4.39
Ti(11)	1.26	1.25	1.25	1.25	1.24
Ti(12)	1.26	1.29	1.27	1.26	1.27



**Movie S1 | *Ab initio* molecular dynamics simulation of rutile TiO<sub>2</sub>(110) in aqueous conditions.** *Ab initio* molecular dynamics trajectory of liquid water on TiO<sub>2</sub>(110) showing that the OH<sub>t</sub> groups, with H atoms depicted in yellow, are stable during the full length of the 50 ps-long AIMD trajectory. It can also be seen that the water molecule in black diffuses between the contact layer and the layer above. The system is composed of 4-trilayers of rutile TiO<sub>2</sub>(110), with a concentration of 1/4 ML of Ti-interstitials lying between the second and third trilayer. The green vertical lines indicate the unit cell used in the simulation, which corresponds to a (4×2) TiO<sub>2</sub>(110) unit cell. The water contact layer consists of a mixture of OH<sub>t</sub> arranged in a (2×1) symmetry and intact water molecules that diffuse in and out of the layer during the time of the simulation. The atoms are colour-coded according to the figures in the manuscript.

## References

1. D. Briggs, M.P. Seah, Practical Surface Analysis, Auger and X-ray Photoelectron Spectroscopy, 2<sup>nd</sup> Ed, Wiley (1990).
2. L. E. Walle, A. Borg, P. Uvdal, A. Sandell, Experimental evidence for mixed dissociative and molecular adsorption of water on a rutile TiO<sub>2</sub>(110) surface without oxygen vacancies. *Phys. Rev. B.* **80**, 235436 (2009)
3. Allegretti, F., O'Brien, S., Polcik, M., Sayago, D. I. & Woodruff, D. P. *Phys. Rev. Lett.* **95**, 226104 (2005).
4. Kurtz, R. L., Stockbauer, R., Madey, T. E., Román, E. & De Segovia, J. Synchrotron radiation studies of H<sub>2</sub>O adsorption on TiO<sub>2</sub>(110). *Surf. Sci.* **218**, 178–200 (1989).
5. Heyd, J.; Scuseria, G. E.; Ernzerhof, M., Hybrid functionals based on a screened Coulomb potential. *J. Chem. Phys.* **118**, 8207 (2003).
6. Perdew, J. P., Burke, K., Ernzerhof, M., Generalized Gradient Approximation Made Simple. *Phys. Rev. Lett.* **77**, 3865 (1996).
7. Morgan, B. J., Watson, G. W. A DFT+U description of oxygen vacancies at the TiO<sub>2</sub> rutile(110) surface. *Surf. Sci.* **601**, 5034 (2007).
8. Luzar, A, Chandler, D. Hydrogen-bond kinetics in Liquid Water. *Nature*, **379**, 55 (1996).

9. Guidon, M., Hutter, J. and VandeVondele, J. Auxiliary density matrix methods for hartree–fock exchange calculations. *J. Chem. Theor. Comput.* **6**(8), 2348-2364 (2010).
10. Guidon, M. Hutter, J. and VandeVondele, J. Robust Periodic Hartree–Fock Exchange for Large-Scale Simulations Using Gaussian Basis Sets. *J. Chem. Theor. Comput.* **5**(11) 3010-3021 (2009).
11. Spreafico, C., and VandeVondele, J. Excess Electrons and Interstitial Li Atoms in TiO<sub>2</sub> Anatase: Properties of the (101) Interface. *J. Phys. Chem. C* **119**(27) 15009-15018 (2015).
12. Henkelman, G., Uberuaga, B. P., Jónsson, H. A climbing image nudged elastic band method for finding saddle points and minimum energy paths. *J. Chem. Phys.* **113**(22) 9901-9904 (2000).
13. Cabailh, G. *et al.* Geometric structure of TiO<sub>2</sub>(110)(1×1): Achieving experimental consensus. *Phys. Rev. B* **75**, 241403 (2007).